Inclusion Characterization in Aluminum-Deoxidized Special Steel with Certain Sulfur Content Under Combined Influences of Slag Refining, Calcium Treatment, and Reoxidation

ZE-WANG HOU, MIN JIANG, EN-JIAO YANG, SHENG-YA GAO, and XIN-HUA WANG

Inclusions in Al-killed steel with [S] of about 0.0060 to 0.0070 mass pct were characterized and discussed, evaluating the combined effects of basic slag refining and Ca treatment in ladle, together with reoxidation of liquid steel in casting tundish. Inclusions were changed from Al_2O_3 to $MgO\text{-}Al_2O_3$ spinel and then to $MgO\text{-}Al_2O_3\text{-}CaO$ during basic slag refining. After Ca treatment, many $(MgO\text{-}Al_2O_3)$ + CaS inclusions were formed, featuring the coexistence of $MgO\text{-}Al_2O_3$ and CaS to form a dual-phased structure. In the following Ar blowing, the number density of $(MgO\text{-}Al_2O_3)$ + CaS inclusions and pure CaS increased obviously, which implied that [Ca] preferentially reacted with [S] rather than [O] in steel. Reoxidation in casting tundish caused the pickup of oxygen in steel, and the rise of total oxygen (T.O) was 0.0002 mass pct; even 55t steel has been poured. As a result, the content of CaO in inclusions increased and $MgO\text{-}Al_2O_3\text{-}CaO$ inclusions were formed again. Thermodynamic calculations revealed that the driving force was strong for the formation of CaS-based inclusions. Higher carbon content in steel would help to reduce oxygen content while enhancing the activity of [S] in steel, which further stabilized the existence of CaS-based inclusions. Therefore, inclusions were mostly the solid $(MgO\text{-}Al_2O_3)$ + CaS dual-phase ones, without the formation of liquid calcium aluminates. Contents of CaS and CaO in inclusions were affected by the [mass pct S]/[mass pct O] ratio, which was calculated as about 4.58 K and 5.34 K at 1873 K and 1823 K, respectively. This finding implied that lower oxygen was not favorable to prevent the solid inclusions in the calcium treatment of high carbon special steel.

https://doi.org/10.1007/s11663-018-1365-x

I. INTRODUCTION

SPECIAL steels were widely used as bearings, gearings, axis, wires, *etc*. in infrastructures and manufacturing industry. Nonmetallic inclusions are often observed as origins of various problems during the production, fabrication, and service of steel. To improve productivity and performances of steels, number, size, chemistry, *etc*. of inclusions should be strictly controlled.

Using Al deoxidation and basic slag refining, oxygen in steel can be reduced to a very low level. The advantage of this technical choice is that the number of inclusions can be greatly decreased. However, the disadvantage is that high melting point inclusions, such as Al_2O_3 or $MgO\text{-}Al_2O_3$, can be easily formed, to reduce castability and the antifatigue property of steel.[1–12] To minimize the negative effects of those inclusions, calcium treatment was often applied to modify them into low melting point calcium aluminate or calcium magnesia aluminate.[13–32] However, formation and evolution of inclusions in Ca treatment are very complex and low melting point inclusions are not absolutely formed.[15,17,18,21,23,32,37–45]

According to the $CaO\text{-}Al_2O_3$ binary phase diagram, calcium aluminates can be reversibly changed between solid and liquid state with the variations of CaO contents. It was widely accepted that modification of Al_2O_3 by [Ca] during Ca treatment followed the unreacted core model, and accumulation of CaO in inclusions against reaction time contributed to the

ZE-WANG HOU, MIN JIANG, EN-JIAO YANG, SHENG-YA GAO and XIN-HUA WANG are with the School of Metallurgical and Ecological Engineering, University of Science and Technology Beijing, Beijing City, P.R. China. Contact e-mail: jiangmin@ustb.edu.cn
Manuscript submitted November 8, 2017.
Article published online August 1, 2018.

formation of liquid calcium aluminate.[25,26,43] Compared to Al_2O_3, modification of spinel is more difficult. Because Mg in inclusion should be reduced by [Ca] and diffusion of the reduced Mg to inclusion surface would be the limiting step, incomplete modification of spinel can occur, especially when they are large in size. In this case, inclusion would be featured by a semiliquid/liquid calcium aluminate surface layer surrounding an unreacted spinel core.[46] According to Pretorius *et al.*, effective modification of spinel by Ca treatment involves two steps, *viz*. reacting with [Ca] and keeping the reaction, in which low oxygen content in steel is very important.[20] Second, CaS inclusions can be easily formed in Ca treatment. CaS can exist as singular particles or clusters and it can also coexist with calcium aluminates/calcium magnesia aluminates as oxy-sulfides or together with MnS as (Ca, Mn)S.[32–36] Verma *et al.* also found CaS can transiently coexist with spinel or Al_2O_3 and further react with Al_2O_3 and spinel to shift them into liquid inclusions.[17–19] Moreover, CaO-CaS-type inclusions can be formed if strong Ca treatment is applied (intensive calcium addition).[15,23,47]

Optimal steel chemistry is very important to inclusion modification in Ca treatment. Previous works revealed that total oxygen (T.O), [Ca], [S], and [Al] in steel comprehensively contributed to the formation and changes of inclusions in Ca treatment. For example, Numata *et al.* reported that Al_2O_3 was initially changed into CaO-Al_2O_3-(low CaS) and then into CaO-Al_2O_3-(high CaS). Further, this evolution routine was reversible with the vaporization of [Ca].[44] Holappa *et al.* found that the "window" for targeting liquid inclusions was narrower at decreased T.O and constant [S] contents, while the expected [Ca] to target liquid inclusions was lower. At constant T.O content, liquid inclusions were more difficult to form at increased [S] content.[41] Jung *et al.* predicted and explained the formation of inclusions in Ca treatment by systematical thermodynamic calculations.[48] They found the mass ratio of CaO/CaS in inclusions was larger if the inclusions just before Ca treatment were initially Al_2O_3. As is known, the vaporization tendency of Ca is very strong during Ca treatment. As a result, the formed inclusions were metastable with the changes of [Ca] in steel. Further, there would be reversible evolutions among CaO-CaS, CaO-Al_2O_3-CaS, and CaS-Al_2O_3 during Ca treatment in low sulfur steel.[44,49]

Despite the preceding achievements and progress, deeper insight on changes of inclusions in Ca treatment is still needed. First, modification of inclusions in Ca treatment was usually under the dual-folding influences of both steel-slag chemical reactions and the Ca treatment operation. Second, reoxidation of molten steel often occurred in practice and the caused oxygen pickup has an important influence on inclusion. However, discussion on this topic was far from enough. Moreover, previous studies on modification of inclusions in Ca treatment were mostly for low carbon steel and much less for high carbon steel melts, especially with higher sulfur contents. Therefore, evolution of inclusions under combined influences of secondary refining, Ca treatment, and reoxidation was investigated in the present study for Al-deoxidized high carbon special steel containing certain sulfur content.

II. EXPERIMENTS AND ANALYSIS

Industrial trials were carried out in a special steel plant. [C], [Si], and [Mn] contents in the commercial steel were 0.87, 0.27, and 0.72 mass pct, respectively. The steelmaking process was composed of hot metal pretreatment, basic oxygen furnace, ladle furnace (LF), Ca treatment, Ar bubbling, and bloom casting. Sampling plans of steel and slag are listed in Table I. Hot rolling coil was also sampled for inclusion inspection.

Chemical compositions of the slag were measured by an X-ray fluorescence spectrometer. Contents of [C], [S], and T.O in steel were obtained by the infrared absorption method. [Mn], [Mg], [Si], [Al], and [Ca] were analyzed by the induction coupled plasma–atomic emission spectrometry machine. While [N] content in steel was measured by the thermal conduction method, steel samples were ground and mirror polished for inclusion inspection under an automatic scanning electron microscope (SEM)–energy-dispersive spectroscope machine (ASPEX explorer) and morphology, size, chemistry, *etc*. of inclusions were obtained.

III. RESULTS AND DISCUSSION

A. *Chemical Compositions of Steel and Slag Samples*

Chemical compositions of steel samples are listed in Table II. T.O was decreased from 0.0029 to 0.0010 mass pct during LF refining. With Ca treatment and Ar bubbling, it was further reduced to 0.0008 and 0.0007

Table II. Chemical Compositions of Steel Samples (Mass Percent)

Steel	S	N	T.O	Al	Ca	Mg
1	0.0070	0.0027	0.0029	0.057	0.0001	0.0003
2	0.0060	0.0027	0.0010	0.049	0.0004	0.0004
3	0.0060	0.0029	0.0008	0.050	0.0025	0.0005
4	0.0060	0.0030	0.0007	0.044	0.0023	0.0006
5	0.0060	0.0043	0.0009	0.040	0.0018	0.0005

Table I. Samplings in Steelmaking and Casting

Sample 1	Sample 2	Sample 3	Sample 4	Sample 5
LF 15 min	LF departure	after Ca treatment (Ar bubbling 3 min)	after Ca treatment (Ar bubbling 16 min)	tundish 55t steel was cast

Table III. Chemical Compositions of Slag Samples (Mass Percent)

Slag	CaO	SiO_2	Al_2O_3	MgO	FeO	MnO	CaO/SiO_2	FeO + MnO
1	63.46	15.25	15.97	5.47	2.46	0.79	4.2	3.96
2	71.64	15.85	13.42	4.38	0.23	0.11	4.5	0.41
3	69.90	15.88	11.82	4.18	0.47	0.10	4.4	0.70
4	68.88	16.84	12.73	4.29	0.22	0.09	4.1	0.37
5	30.39	32.53	10.47	12.64	3.00	0.81	0.9	3.81

mass pct, respectively. Dissolved [Al] was continuously decreased from 0.057 to 0.040 mass pct during refining and casting. Because of Ca treatment, [Ca] was increased from 0.0004 mass pct at the end of LF to 0.0025 mass pct after 3 minutes of Ar bubbling. Fluctuations of [N] were controlled within 0.0002 mass pct during LF refining and Ca treatment. However, [N] was increased by 0.0013 mass pct in tundish together with a pickup of T.O about 0.0002 mass pct, indicating the occurrence of reoxidation to liquid steel.

As shown in Table III, top slag basicity of LF was about 4.1 to 4.5 while (FeO + MnO) contents were decreased from initially 3.96 to about 0.37 mass pct at the end of LF refining. Tundish flux had lower basicity of about 0.9 and much higher (FeO + MnO) content about 3.8 mass pct.

B. *Characterization of Inclusions*

1. *Observed typical inclusions*

Typical inclusions are given in Figure 1, in which the arrows mark the EDS points, while data in the labeled tables are weight percentages of the detected elements. Features of inclusions can be briefly described as follows.

(1) After 15 minutes of LF refining, inclusions were mainly Al_2O_3 and some MgO-Al_2O_3. Al_2O_3 was either in blocky shape smaller than 10 μm or in cluster shape with sizes about several tens of microns.
(2) At the end of LF refining, inclusions were mainly changed into MgO-Al_2O_3-CaO, MgO-Al_2O_3, and a few (MgO-Al_2O_3-CaO)-CaS.
(3) Inclusions were modified into (MgO-Al_2O_3) + CaS and (MgO-Al_2O_3-CaO)-CaS after Ca treatment and 3 minutes of Ar blowing. (MgO-Al_2O_3) + CaS inclusions were featured by much higher CaS content and appeared in a dual-phase structure composed of spinel and CaS.
(4) Most of the inclusions were (MgO-Al_2O_3) + CaS after Ar bubbling for 16 minutes. Particularly, pure CaS inclusions were produced.
(5) In casting tundish, most of the inclusions were still (MgO-Al_2O_3) + CaS. However, the content of CaO in inclusions obviously increased. MgO-Al_2O_3-CaO and (MgO-Al_2O_3-CaO)-CaS inclusions appeared again.
(6) Notably, the dual-phased (MgO-Al_2O_3) + CaS inclusions were slightly changed all the time. This finding implied that further chemical reaction between CaS and spinel was difficult to occur.

Figure 2 shows SEM mappings of (MgO-Al_2O_3-CaO)-CaS and (MgO-Al_2O_3) + CaS inclusions. As can be seen, CaS precipitated on the surface of (MgO-Al_2O_3-CaO)-CaS inclusions while CaO enriched in the subsurface layer and MgO-Al_2O_3 remained as the core. (MgO-Al_2O_3) + CaS inclusions are featured by MgO-Al_2O_3 in the center wrapped with a much thicker layer of CaS.

2. *Changes in inclusion composition in ladle refining, Ca treatment, and casting tundish*

Contents of Al, Ca, Mg, S, *etc*. in inclusions obtained by EDS were converted into Al_2O_3, CaO, MgO, CaS, *etc*. and are plotted in Figure 3, with the assumption that enough oxygen was contained in the inclusions.

(1) After 15 minutes of LF refining, inclusions were mostly pure alumina and MgO-Al_2O_3 with MgO less than 20 mass pct. With the procession of refining, CaO and MgO contents in inclusions increased.
(2) Three minutes after Ar blowing (Ca treatment was used), an impressive increase of CaS in inclusions was witnessed but CaO content changed slightly.
(3) Sixteen minutes after Ar blowing, content of CaS in inclusions further increased. However, the content of CaO in inclusions was constantly low and slightly changed.

The average composition change of inclusions is given in Figure 4. As can be seen, CaO in inclusions was always much lower than other components. Therefore, composition distribution of the detected inclusions can be approximately as shown in Figure 5. As indicated, the mass ratio of MgO to Al_2O_3 in inclusions was about 0.3 before Ca treatment. It increased to about 0.5 after Ca treatment and negligibly changed afterward, which implied that spinel is slightly modified despite Ca treatment.

After Ca treatment, the number density of inclusions sharply increased from 1.6/mm^2 at the end of LF refining to 9.5 and 23.9/mm^2 after 3 and 16 minutes of Ar blowing, respectively. Moreover, changes in number density were distinctive for different types of inclusions, as shown in Figure 6, which meant that [Ca] preferentially reacted with [S] during Ca treatment to produce (MgO-Al_2O_3) + CaS and pure CaS. Their number density decreased while that of MgO-Al_2O_3-CaO increased again to 0.2/mm^2 in tundish, indicating the occurrence of [Ca]-[O] reaction in steel because of the oxygen pickup in reoxidation.

C. *Discussions on Evolution of Inclusions*

1. *Qualitative analysis on the influences of slag, refractory, and Ca treatment*

Under slag refining, complex chemical reactions occurred among slag-steel-inclusion refractory. Reactions [1] and [2] between basic slag and added Al can occur, in which Mg and Ca were reduced from slag and

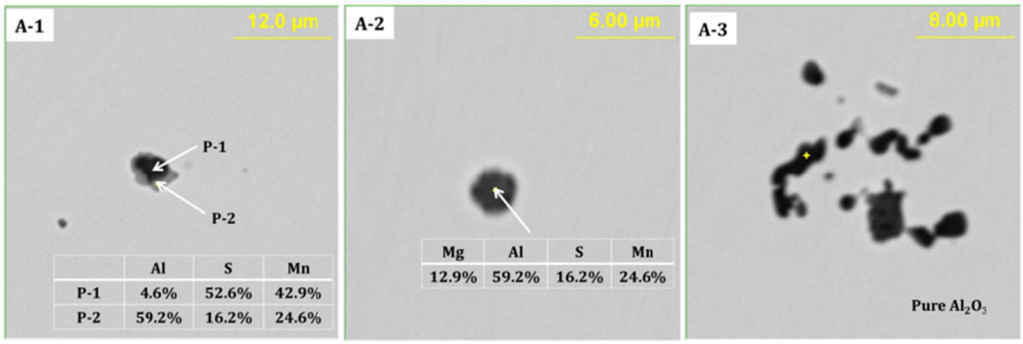

(a)

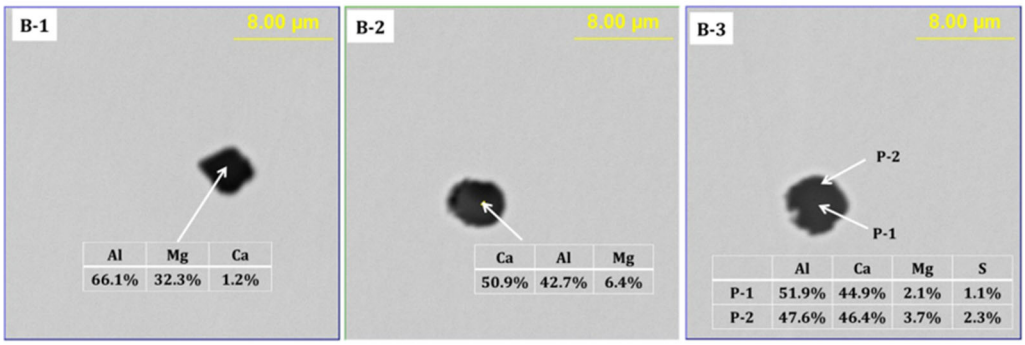

(b)

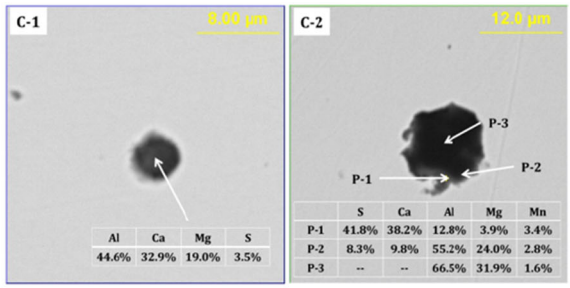

(c)

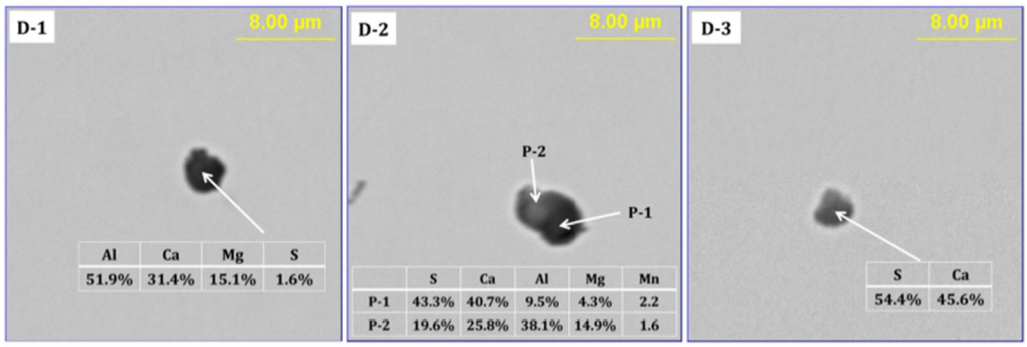

(d)

Fig. 1—Typical inclusion in steelmaking and casting tundish: (*a*) 15 min after LF refining, (*b*) at the end of LF refining, (*c*) after calcium treatment and Ar bubbling for 3 min, (*d*) after calcium treatment and Ar bubbling for 16 min, (*e*) in the casting tundish, and (*f*) inclusion in hot-rolled coil.

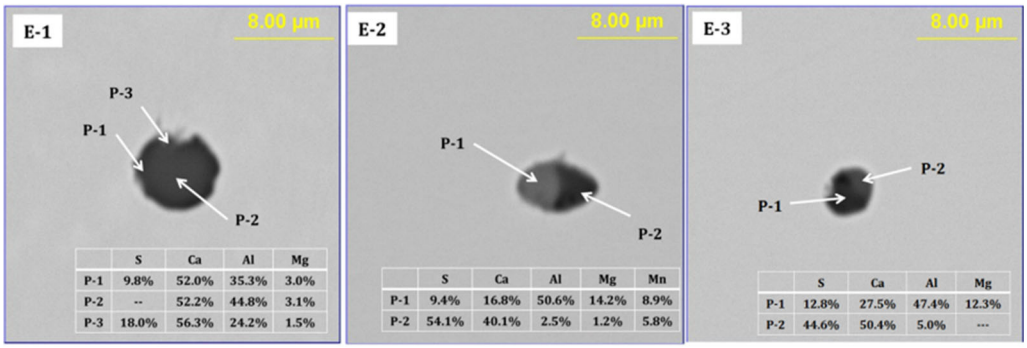

(e)

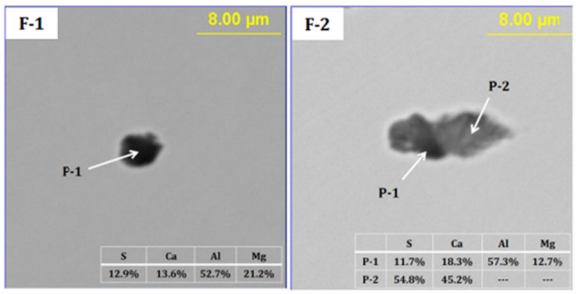

(f)

Fig. 1—continued.

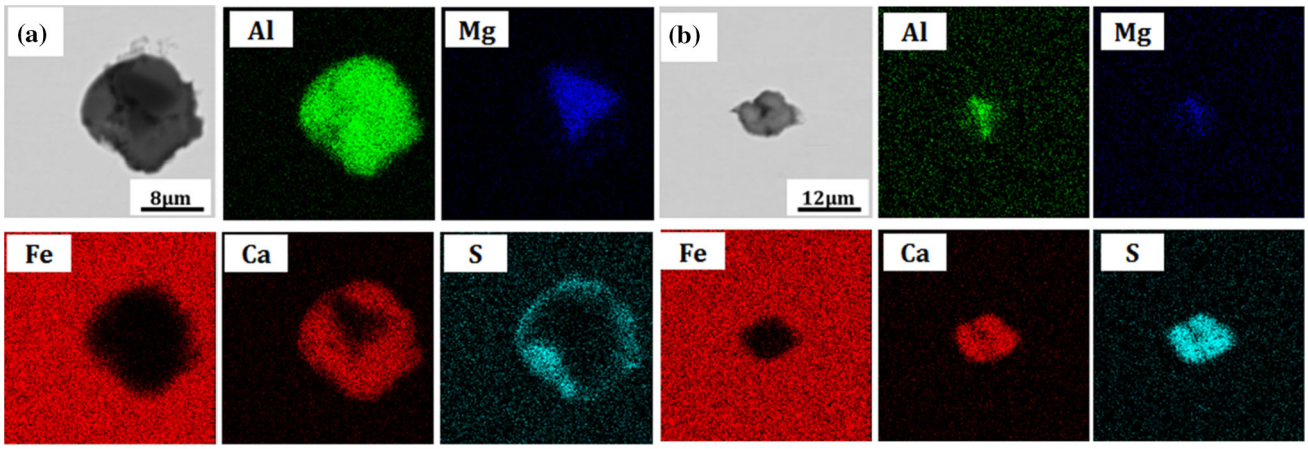

Fig. 2—SEM mappings of different coexistence states of CaS in complex inclusions: (*a*) CaS in (MgO-Al_2O_3-CaO)-CaS and (*b*) CaS in (MgO-Al_2O_3) + CaS inclusions.

supplied to molten steel. The brackets and parentheses in the equations denote the components in steel and slag, respectively.

$$2[Al] + 3(MgO) = (Al_2O_3) + 3[Mg] \quad [1]$$

$$2[Al] + 3(CaO) = (Al_2O_3) + 3[Ca] \quad [2]$$

In MgO-C refractory of the ladle, Reactions [3] and [4] might occur under the heating of the electrical arc of LF, where the braces in the equations denote the components in refractory while the symbol "↑" denotes the gas phase. In practice, this reaction was difficult to occur without vacuum atmosphere. Therefore, the slag-steel reaction was considered as the main source for [Mg] in steel.

$$\{MgO\} + \{C\} = Mg\uparrow + CO\uparrow \quad [3]$$

$$Mg\uparrow = [Mg] \quad [4]$$

By contrast, there was another source of [Ca] in steel. In Ca treatment, the supply of [Ca] to steel can be expressed by Reactions [5] and [6]. The added Ca wire

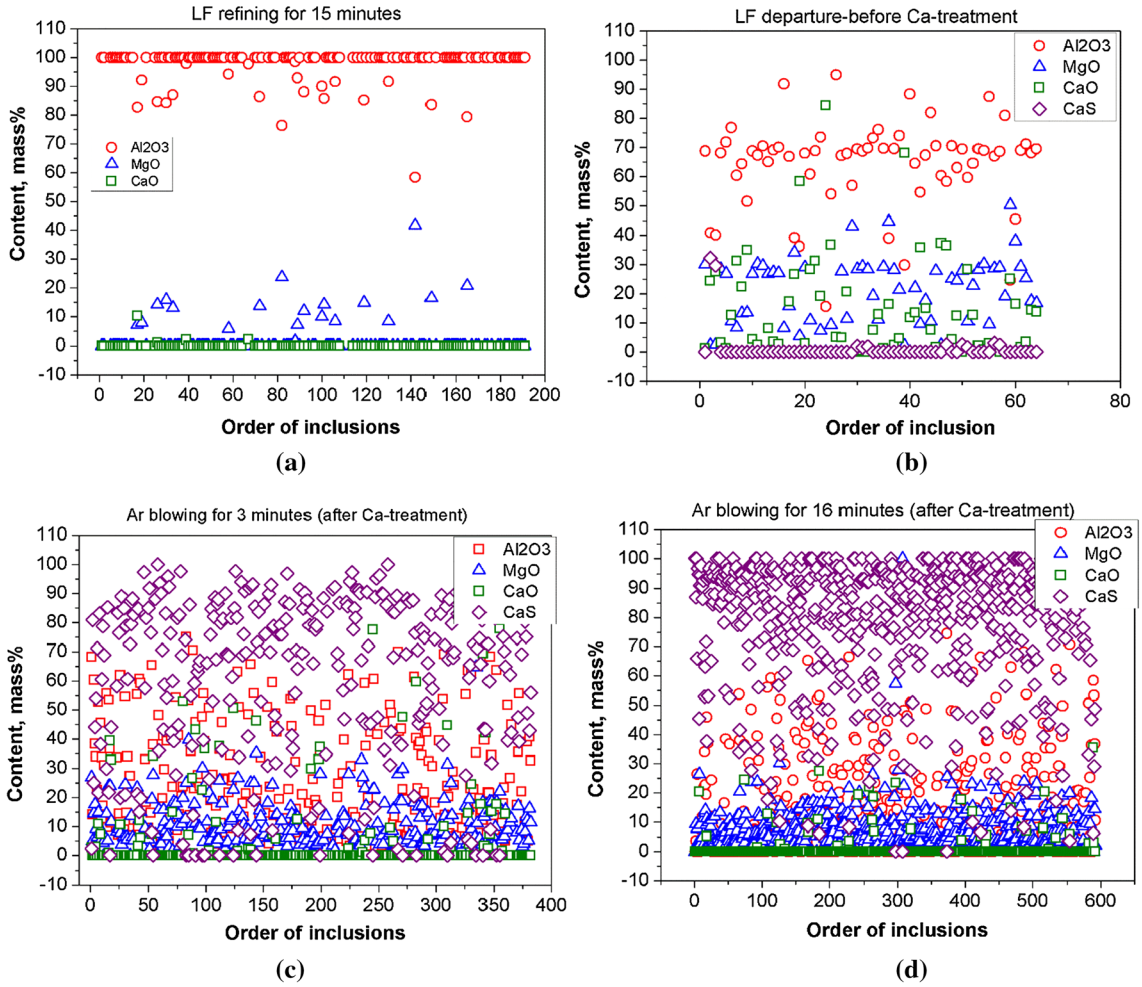

Fig. 3—Composition changes of inclusions during refining, Ca treatment, and Ar bubbling: (*a*) after 15 min LF refining, (*b*) LF departure/before Ca treatment, (*c*) Ar blowing for 3 min, and (*d*) Ar blowing for 16 min.

would be initially melted or vaporized as gas state before dissolving into steel, where Ca_l and Ca ↑ denoted the liquid and gas phases of calcium, respectively.

$$Ca = Ca_l \text{ or } Ca \uparrow \quad [5]$$

$$Ca_l \text{ or } Ca \uparrow = [Ca] \quad [6]$$

The rise of [Mg] and [Ca] would greatly affect inclusions in steel. In LF refining, changes of inclusions from Al_2O_3 into $MgO{\cdot}Al_2O_3$ and $MgO\text{-}Al_2O_3\text{-}CaO$ before Ca treatment were mainly caused by slag-steel reactions. This topic has been intensively discussed in recent years, including in a series of works by the present authors.[14] Therefore, it is not discussed too much here.

During Ca treatment, modification of spinel can be expressed by Reaction [7] while formation of CaS can be expressed either by Reactions [8] or [9]. Occurrence of Reaction [8] implied desulfurization of steel by slag, while Reaction [9] indicated the formation of CaS by the reaction of [Ca] and [S] inside molten steel. As given in Table II, [S] in steel slightly changed in refining and casting. Therefore, large formation of CaS after Ca treatment in the present study should be attributed to Reaction [9].

$$[Ca] + \left(x + \frac{1}{y}\right)(Al_2O_3 \cdot yMgO) = \left(CaO \cdot \left(x + \frac{1}{y}\right)Al_2O_3 \cdot x(y)MgO\right) + [Mg] \quad [7]$$

$$3(CaO) + 2[Al] + 3[S] = (Al_2O_3) + 3(CaS) \quad [8]$$

$$[Ca] + [S] = (CaS) \quad [9]$$

2. *Thermodynamic calculations on inclusions*

Thermodynamic calculations were done to evaluate the formation and changes of inclusions. Involved chemical reactions and data are listed in Table IV. Interaction coefficients used in the thermodynamic calculations were indirectly referred from previous

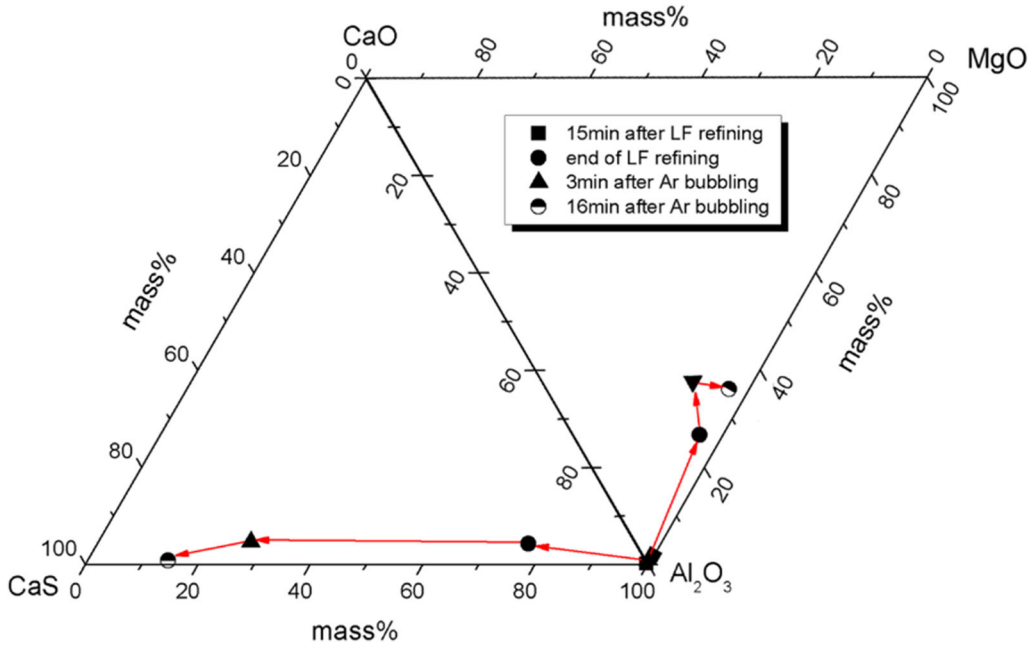

Fig. 4—Average composition changes of inclusions in refining, Ca treatment, and Ar bubbling.

literature[15,53] and were mostly summarized by Suito and Inoue in 1996.[53] Activity of solute in steel was calculated by Eqs. [10] and [11], where e_i^j is the interaction coefficient of element j to i, [mass pct j] is the mass content of j, and f_i is the activity coefficient of i.

$$\lg f_i = \sum e_i^j [\text{mass pct } j] \quad [10]$$

$$a_i = f_i \cdot [\text{mass pct i}] \quad [11]$$

Equation [12] can be deduced to estimate the formation of CaS in Reaction [9], where a_{CaS} was the activity of CaS and was taken as unity; f_s and f_{Ca} were the activity coefficients of [Ca] and [S] in steel, respectively; ΔG_9° was the standard formation Gibbs free energy; T was the temperature in Kelvin; and R was the ideal gas constant. Two temperatures (1823 K and 1873 K) were used because the refining temperature in practice was within this range. As shown in Figure 7, CaS was largely formed in Ca treatment and its formation would be much easier at lower temperature, which explained the preferential reaction between [Ca] and [S] to produce CaS.

$$[\text{mass pct Ca}][\text{mass pct S}] = \frac{a_{CaS}}{f_S \cdot f_{Ca}} \cdot \exp\left(\frac{-\Delta G_9^\circ}{RT}\right) \quad [12]$$

Reaction [13] was obtained based on Reactions [9] and [11]. Further, Eqs. [14] and [15] were deduced, where ΔG_{13}° was the standard formation Gibbs free energy; T was the Kelvin temperature; K_{13} was the equilibrium constant; f_S and f_O were the activity coefficients of [S] and [O] in steel, respectively; and a_{CaO} and a_{CaS} were the activities of CaO and CaS in inclusions, respectively. Because f_S, f_O, and K_{13} were constants at the given conditions, they can be merged together as a constant A in Eq. [15]. As can be seen, variations of CaS and CaO in inclusions depended on the [mass pct S]/[mass pct O] ratio in steel. The increase of oxygen would result in the rise of CaO content in inclusions. When competition between [O] and [S] to react with [Ca] approached chemical equilibrium, a critical [mass pct S]/[mass pct O] ratio was calculated about 4.58 K and 5.34 K at 1873 K and 1823 K, respectively.

$$(\text{CaS}) + [\text{O}] = (\text{CaO}) + [\text{S}] \quad [13]$$

$$\Delta G_{13}^\circ = -87,467 + 20.6T \quad [14]$$

$$\frac{a_{CaS}}{a_{CaO}} = \frac{K_{13} \times f_S}{f_O} \times \frac{[\text{mass pct S}]}{[\text{mass pct O}]} = A \times \frac{[\text{mass pct S}]}{[\text{mass pct O}]} \quad [15]$$

It can be observed in Table II that [mass pct S]/T.O ratios in experiments were about 6 to 7 from the end of LF to casting tundish. Because the steel melt was under Al deoxidation and basic slag refining, [mass pct O] was very low and should be much smaller than T.O content. Hence, [mass pct S]/[mass pct O] ratios should be larger than 6 to 7, which meant that CaS was more stable than CaO in inclusions. On the other hand, measured pickups of T.O and [N] in tundish owed to reoxidation were 0.0002 and 0.0013 mass pct, respectively; even 55 tons of steel has been poured. As the rise of [N] originated from air and was slightly affected

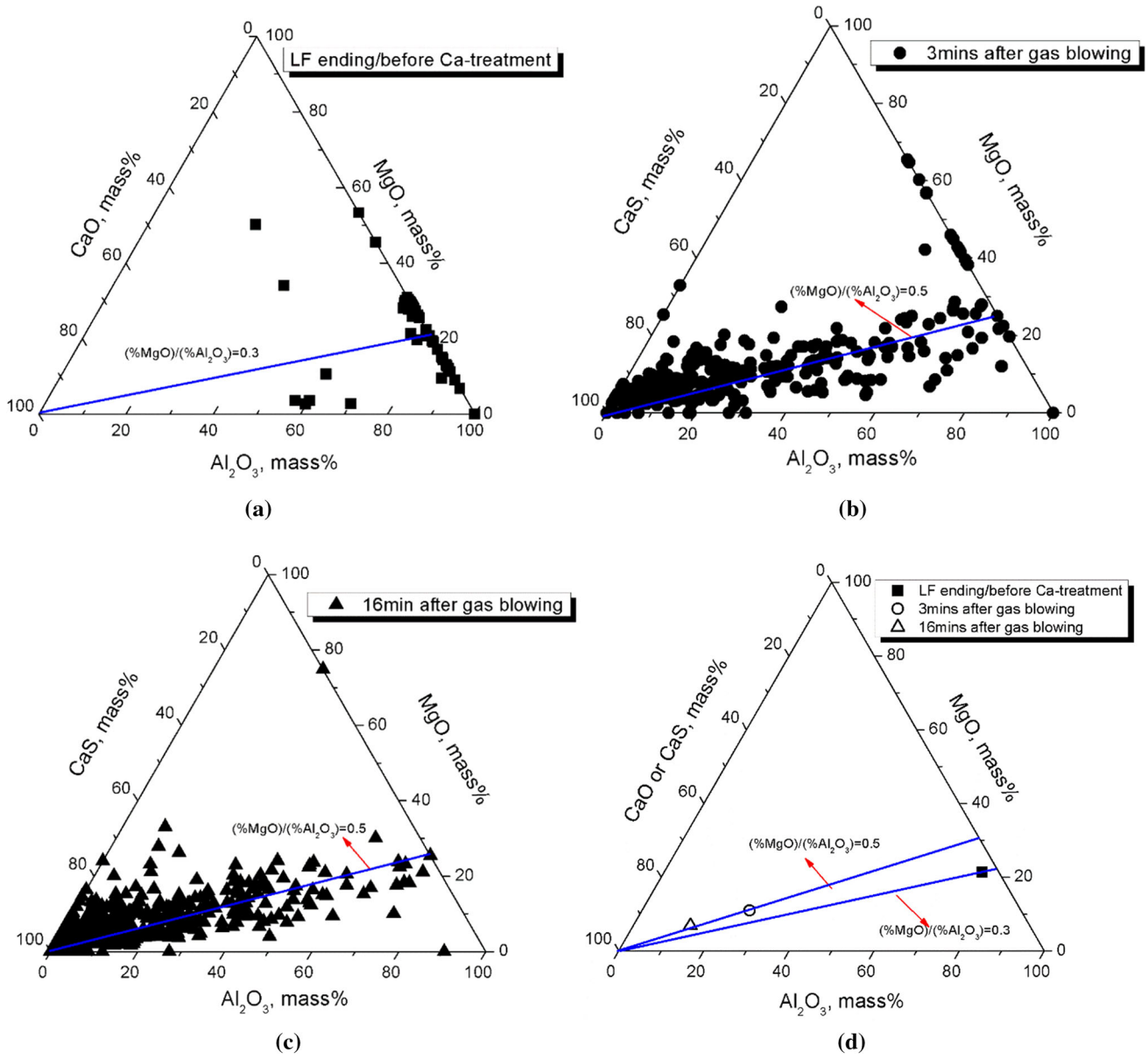

Fig. 5—Composition changes of inclusions during Ca treatment, Ar bubbling, and casting: (*a*) LF ending/before Ca treatment, (*b*) 3 min after Ar blowing, (*c*) 16 min after Ar blowing, and (*d*) in casting tundish.

by inclusion floatation, oxygen absorbed from air can be estimated to be about 0.0004 mass pct, assuming that the mole ratio of N_2 to O_2 in air was 78 to 21 pct. Except the exposure to air, reoxidation of steel can also be caused by the reactions among steel ([Al]) with FeO, MnO, and SiO_2 in tundish flux. Moreover, efficient inclusion floatation in tundish would partially offset the oxygen pickup. Considering these factors, it was reasonably inferred that actual pickup of oxygen was higher than the measured 0.0002 mass pct; *viz*. the driving force of Reaction [16] in the experiment should be stronger than calculation. Reoxidation was the reason for the rise of CaO content in inclusions in tundish. As a result, $MgO\text{-}Al_2O_3\text{-}CaO$ inclusions were formed again and the number of $MgO\text{-}Al_2O_3\text{-}CaO\text{-}CaS$ increased.

In many previous works, effective modification of spinel by Ca treatment was observed. However, spinel was slightly changed in the present study. To explain this phenomenon, thermodynamic equilibrium on the modification spinel in Ca treatment in the present study was evaluated and compared to the recent works of Verma *et al*.[19] Assuming the formed liquid phase was $12CaO{\cdot}7Al_2O_3$, Reaction [16] can be obtained based on Reactions [9] through [12]. Then, thermodynamic calculation can be carried out to obtain Table V and Figure 8, in which activities of CaS and $C_{12}A_7$ were taken as unity while the activity of Al_2O_3 in spinel was taken as 0.47. As can be seen, modification of spinel into liquid calcium aluminate was much more difficult in the present study.

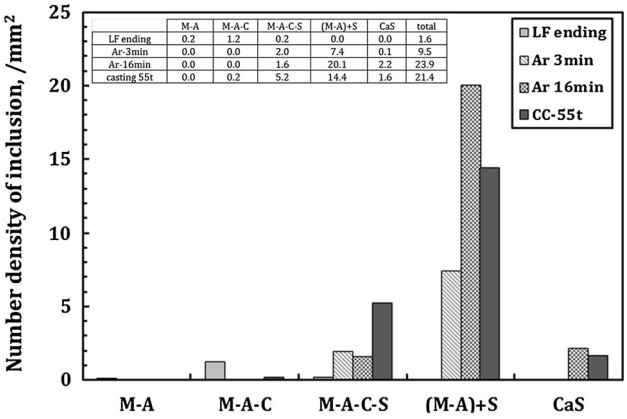

Fig. 6—Changes of inclusion number density in refining, Ca treatment, and casting. (Note M, A, C, and S in the figure stand for MgO, Al_2O_3, CaO, and CaS in inclusion.).

Table IV. Related Chemical Reactions and Gibbs Free Energy

Chemical Reaction	Gibbs Free Energy	Reactions
[Ca] + [S] = (CaS)	− 542,531 + 124.15T[50]	[9]
2[Al] + 3[O] = (Al_2O_3)	− 1,225,417 + 393.8T[50]	[10]
[Ca] + [O] = (CaO)	− 629,998 + 144.75T[51]	[11]
12(CaO) + 7(Al_2O_3) = 12CaO·7Al_2O_3	617,977 − 612T[52]	[12]

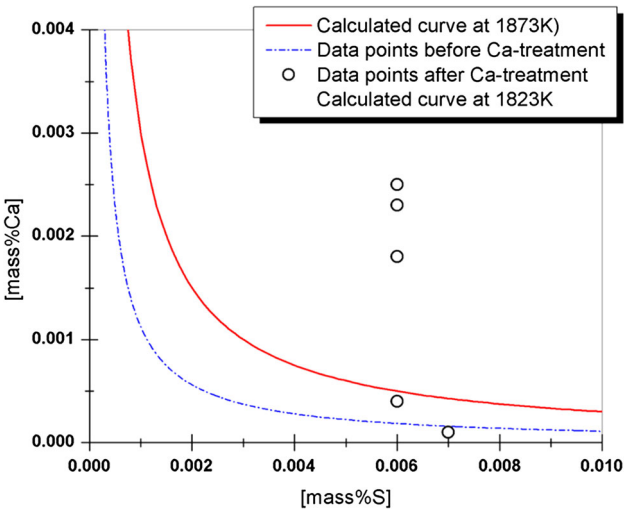

Fig. 7—Thermodynamic equilibrium curve between [Ca] and [S] in steel.

$$11(Al_2O_3)_{spinel}+12(CaS) = (12CaO \cdot 7Al_2O_3) + 8[Al] + 12[S] \quad [16]$$

The main reason was attributed to the great influence of [C] content on the activity coefficients f_O and f_S.

Table V. Estimated Equilibrium Value of $[Al]^2 \cdot [S]^3$ in Steel Melts

	1873 K	1823 K
Present study	6.20×10^{-8}	8.67×10^{-9}
Study of Verma *et al.*	1.79×10^{-7}	2.51×10^{-8}

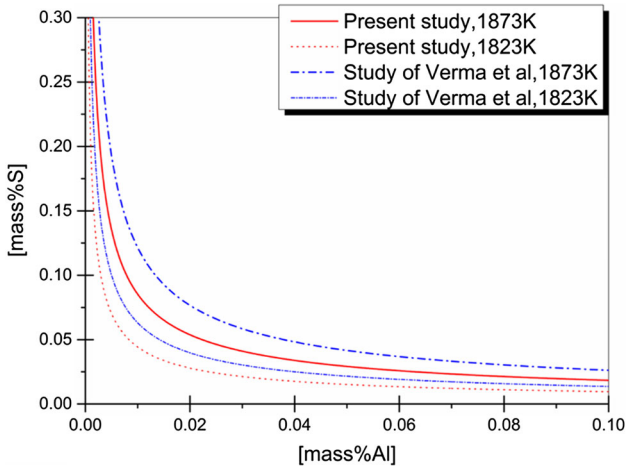

Fig. 8—Effects of [mass pct Al] and [mass pct S] on modification of spinel into liquid calcium aluminate by CaS.

From previous literature,[53] it is known that [C] has strong interaction with [S] and [O] in steel. [C] content in steel was 0.87 mass pct in the present study, while that in the experiments of Verma *et al.* was only 0.06 mass pct. As a result, lower dissolved oxygen can be expected in the present study. Moreover, it would contribute to the higher activity of [S] in steel, causing not only easier formation but also more stable existence of CaS than CaO. Therefore, spinel always coexisted with CaS as (MgO-Al_2O_3) + CaS inclusions in the present study, and further chemical reactions between them were hard to occur with the dual-phased structure well kept.

IV. CONCLUSIONS

Formation and changes of inclusions in low oxygen special steel with certain sulfur content were studied, considering the combined influences of refining, Ca treatment, and reoxidation. It was found that inclusions were under continuous evolutions from refining, Ar blowing, and continuous casting. Based on the results obtained, the following conclusions were drawn.

1. During ladle refining, inclusions were mainly changed from Al_2O_3 to MgO-Al_2O_3 and MgO-Al_2O_3-CaO. Some (MgO-Al_2O_3-CaO)-CaS inclusions were also observed, featuring MgO-Al_2O_3-CaO as the core surrounded by a precipitated CaS layer. After Ca

treatment, CaS was largely produced and coexisted with spinel to form dual-phased ($MgO\text{-}Al_2O_3$) + CaS inclusions, often with spinel in the center with CaS layer wrapped outside.

2. With the procession of Ar blowing after Ca treatment, the number of ($MgO\text{-}Al_2O_3$) + CaS inclusions sharply increased and singular CaS inclusions were also produced. Reoxidation of steel in tundish resulted in the rise of CaO content in inclusions. As a result, $MgO\text{-}Al_2O_3$-CaO inclusions were formed again in steel and the number of ($MgO\text{-}Al_2O_3$-CaO)-CaS indicated an increase. The content of CaS and CaO in inclusions was closely related to the mass ratio of [mass pct S]/[mass pct O] in steel, which implied that too low oxygen content in steel is not favorable to prevent solid inclusions. Further, the critical [mass pct S]/[mass pct O] when equilibrium between CaS and CaO was established was calculated to be about 4.58 K and 5.34 K at 1873 K and 1823 K, respectively
3. The driving force was strong for the formation of CaS. High [C] content in steel ever intensive its stable existence because higher [C] content would enhance the activity of [S] while helping to reduce the [O] content in steel. This accounted for the large formation and stable existence of CaS in the present work. Because of a very strong combination of [S] and [Ca], spinel was slightly modified during Ca treatment and the two coexisted stably with CaS to the form the ($MgO\text{-}Al_2O_3$) + CaS dual-phase inclusions. The increase of oxygen content would break the formation equilibrium of CaS, because it would help to produce CaO-contained inclusion. The competition of [S] and [O] in reacting with [Ca] was closely related to the [mass pct S]/[mass pct O] ratio in steel, which was estimated to be about 4.58 K and 5.34 K at 1873 K and 1823 K, respectively.

ACKNOWLEDGMENT

The authors are thankful for the support of China National Science Funding (Grant No. 51304013) during this research.

REFERENCES

1. C. Shi, X. Chen, H. Guo, Z. Zhu, and X. Sun: *Metall. Mater. Trans. B*, 2013, vol. 44B, pp. 378–89.
2. J.H. Park and H. Todoroki: *ISIJ Int.*, 2010, vol. 50, pp. 1333–46.
3. M. Jiang, X.H. Wang, B. Chen, and W.J. Wang: *ISIJ Int.*, 2008, vol. 48, pp. 885–90.
4. J.H. Park: *Metall. Mater. Trans. B*, 2007, vol. 38B, pp. 657–63.
5. Y. Ehara, S. Yokoyama, and M. Kawakami: *Tetsu-to-Hagané*, 2007, vol. 93, pp. 475–82.
6. J.H. Park and D.S. Kim: *Metall. Mater. Trans. B*, 2005, vol. 36B, pp. 495–502.
7. H. Todoroki and K. Mizuno: *ISIJ Int.*, 2004, vol. 44, pp. 1350–57.
8. H. Todorki and K. Mizuno: *Iron Steelmaker Trans.*, 2003, vol. 61B, pp. 60–68.
9. G. Okuyama, K. Yamaguchi, S. Takeuchi, and K.I. Sorimachi: *ISIJ Int.*, 2000, vol. 40, pp. 121–28.
10. T. Nishi and K. Shinme: *Tetsu-to-Hagané*, 1998, vol. 84, pp. 837–43.
11. H. Itoh, M. Hino, and S. Ban-Ya: *Metall. Mater. Trans. B*, 1997, vol. 28B, pp. 953–56.
12. J.W. Kim, S.K. Kim, D.S. Kim, Y.D. Lee, and P.K. Yang: *ISIJ Int.*, 1996, vol. 36, pp. S140–43.
13. Z. Deng and M. Zhu: *ISIJ Int.*, 2013, vol. 53, pp. 450–58.
14. M. Jiang, X.H. Wang, B. Chen, and W.J. Wang: *ISIJ Int.*, 2010, vol. 50, pp. 95–104.
15. G.W. Yang, X.H. Wang, F.X. Huang, D. Yang, P. Wei, and X. Hao: *Metall. Mater. Trans. B*, 2014, vol. 46B, pp. 145–54.
16. S.F. Yang, J.S. Li, Z.F. Wang, J. Li, and L. Lin: *Metall. Mater. Trans. B*, 2011, vol. 18B, pp. 18–23.
17. N. Verma, P.C. Pistorius, R.J. Fruehan, M. Potter, M. Lind, and S.R. Story: *Metall. Mater. Trans. B*, 2011, vol. 42B, pp. 720–29.
18. N. Verma, P.C. Pistorius, R.J. Fruehan, M. Potter, M. Lind, and S. Story: *Metall. Mater. Trans. B*, 2011, vol. 42B, pp. 711–19.
19. N. Verma, P.C. Pistorius, and R.J. Fruehan: *Iron Steel Technol.*, 2010, vol. 7, pp. 189–97.
20. E.B. Pretorius, H.G. Oltmann, and T. Cash: *Iron Steel Technol.*, 2010, vol. 7, pp. 31–44.
21. M. Lind and L. Holappa: *Metall. Mater. Trans. B*, 2010, vol. 41B, pp. 359–66.
22. A. Ghosh: *Trans. Ind. Inst. Met.*, 2008, vol. 61, pp. 473–75.
23. Y. Ito, S. Nara, Y. Kato, and M. Suda: *Tetsu-to-Hagané*, 2007, vol. 93, pp. 355–61.
24. S.K. Choudhary and S. Chandra: *ISIJ Int.*, 2007, vol. 47, pp. 190–92.
25. J.H. Park, D.S. Kim, and S.B. Lee: *Metall. Mater. Trans. B*, 2005, vol. 36B, pp. 67–73.
26. G. Ye, P. Jonsson, and T. Lund: *ISIJ Int.*, 1996, vol. 36, pp. S105–S108.
27. Y. Kusano, Y. Kawauchi, M. Wajima, K. Sugawara, M. Yoshida, and H. Hayashi: *ISIJ Int.*, 1996, vol. 36, pp. S77–S80.
28. Y. Ito, M. Suda, Y. Kato, H. Nakato, and K. Sorimachi: *ISIJ Int.*, 1996, vol. 36, pp. S148–S150.
29. Y. Higuchi, M. Numata, S. Fukagawa, and K. Shinme: *Tetsu-to-Hagané*, 1996, vol. 82, pp. 671–76.
30. Y. Highchi, M. Numata, S. Fukagawa, and K. Shinme: *ISIJ Int.*, 1996, vol. 36, pp. S151–54.
31. M. Imagumbai and T. Takeda: *ISIJ Int.*, 1994, vol. 34, pp. 574–83.
32. D. Janke, Z. Ma, P. Valentin, and A. Heinen: *ISIJ Int.*, 2000, vol. 40, pp. 31–39.
33. G. Xu, Z. Jiang, and Y. Li: *Metall. Mater. Trans. B*, 2016, vol. 47B, pp. 2411–20.
34. Y. Guo, S.P. He, G. Chen, and Q. Wang: *Metall. Mater. Trans. B*, 2016, vol. 47B, pp. 2549–57.
35. F. Jiang, G. Cheng, G. Qian, Y. Xie, Q. Rui, and L. Yang: *Steel Res. Int.*, 2013, vol. 84B, pp. 554–59.
36. B. Korousic, F. Tehovnik, and B. Arh: *Steel Res.*, 2001, vol. 72, pp. 35–39.
37. N. Verma, P.C. Pistorius, R.J. Fruehan, M.S. Potter, H.G. Oltmann, and E.B. Pretorius: *Metall. Mater. Trans. B*, 2012, vol. 43B, pp. 830–40.
38. C.W. Seo, S.H. Kim, S.K. Jo, M.O. Suk, and S.M. Byun: *Metall. Mater. Trans. B*, 2010, vol. 41B, pp. 790–97.
39. M. Numata and Y. Higuchi: *Tetsu-to-Hagané*, 2011, vol. 97, pp. 259–65.
40. S.K. Choudhary and A. Ghosh: *ISIJ Int.*, 2008, vol. 48, pp. 1552–59.
41. L. Holappa, M. Hämäläinen, M. Liukkonen, and M. Lind: *Iron Steelmaking*, 2003, vol. 30, pp. 111–15.
42. Y. Wang, M. Valdez, and S. Sridhar: *Metall. Mater. Trans. B*, 2002, vol. 33B, pp. 625–32.
43. M. Numata, Y. Higuchi, and S. Fukagawa: *Tetsu-to-Hagané*, 1998, vol. 84, pp. 159–64.
44. B. Ozturk and E.T. Turkdogan: *Met. Sci.*, 1984, vol. 18, pp. 306–09.
45. B. Ozturk and E.T. Turkdogan: *Met. Sci.*, 1984, vol. 18, pp. 299–305.
46. X.W. Zhang, L.F. Zhang, W. Yang, Y. Liu, and Y.C. Dong: *Metall. Mater. Trans. B*, 2017, vol. 48B, pp. 701–12.
47. G.W. Yang and X.H. Wang: *ISIJ Int.*, 2015, vol. 55, pp. 126–33.

48. I.H. Jung, S.A. Decterov, and A.D. Pelton: *ISIJ Int*., 2004, vol. 44, pp. 527–36.
49. G.W. Yang, X.H. Wang, F.X. Huang, W.J. Wang, Y.Q. Yin, and C.X. Tang: *Steel Res. Int*., 2014, vol. 85, pp. 784–92.
50. Steelmaking Data Sourcebook: *The Japan Society for the Promotion of Science*, Gordon & Breach Science Publishers, New York, NY, 1988.
51. G.K. Sigworth and J.F. Elliott: *Met. Sci*., 1974, vol. 8, p. 298.
52. R.H. Rein and J. Chipman: *Trans. TMS-AIME*, 1965, vol. 233, p. 415.
53. H. Suito and R. Inoue: *ISIJ Int*., 1996, vol. 36, pp. 528–36.